JOURNAL OF COMPUTATIONAL PHYSICS 110, 301–309 (1994)

A Self-Correcting Procedure for Computational Liquid Metal Magnetohydrodynamics

HIDEO ARASEKI

Central Research Institute of Electric Power Industry, 1646 Abiko, Abiko-shi, Chiba-ken 270-11, Japan

AND

SHOJI KOTAKE

The Japan Atomic Power Company, 6-1, 1-Chome, Ohtemachi, Chiyoda-ku, Tokyo 100, Japan

Received September 24, 1992

This paper describes a new application of the self-correcting procedure to computational liquid metal magnetohydrodynamics. In this procedure, the conservation law of the electric current density incorporated in a Poisson equation for the scalar potential plays an important role of correcting this potential. This role is similar to that of the conservation law of mass in a Poisson equation for the pressure. Some numerical results show that the proposed self-correcting procedure can provide a more accurate numerical solution of the electric current density than the existing solution procedure. © 1994 Academic Press, Inc.

1. INTRODUCTION

A solution procedure including a Poisson equation for the pressure is the most popular one in a computation of incompressible fluid flow. This procedure was originated by Harlow and Welch [1] and is called the marker-and-cell (MAC) method [2]. Also its variations have been widely used not only in the finite difference method [3–5] but also in the finite element method [6, 7]. The principle of this solution procedure was discussed by Hirt and Harlow [8], and they described it as "the self-correcting procedure."

Now let us see the outline of the self-correcting procedure according to Hirt and Harlow's idea in a computation of incompressible fluid flow [8]. The semi-discretized conservation equations are

$$\mathbf{u}^{n+1} = \mathbf{u}^n + \frac{\Delta t}{\rho}\{-\nabla p^{n+1} + \mathbf{f}^n\} \tag{1.1}$$

$$\nabla \cdot \mathbf{u}^{n+1} = 0, \tag{1.2}$$

where $\mathbf{u}$ is the fluid velocity, p is the pressure, ρ is the fluid density, $\mathbf{f}$ denotes all the other terms such as the convection and the diffusion terms, and the superscript n's mean the time steps. Taking the divergence on both sides of Eq. (1.1) and using Eq. (1.2), we obtain a Poisson equation for the pressure

$$\nabla^2 p^{n+1} = \nabla \cdot \mathbf{f}^n + \frac{\rho}{\Delta t}\nabla \cdot \mathbf{u}^n. \tag{1.3}$$

The final term in the right-hand side of Eq. (1.3), if it is not zero, corrects the pressure field so that the velocity field at the next time step should satisfy Eq. (1.2). The point of the self-correcting procedure lies in keeping the final term, although it could be eliminated in principle. This is the overview of the self-correcting procedure in computational fluid dynamics.

Now let us compare the above equations with Ohm's law

$$\mathbf{J}^{n+1} = \sigma(-\nabla\phi^{n+1} + \mathbf{u}^n \times \mathbf{B}^n) \tag{1.4}$$

and the conservation law of the electric current density

$$\nabla \cdot \mathbf{J}^{n+1} = 0 \tag{1.5}$$

and a Poisson equation for the scalar potential derived from Eqs. (1.4) and (1.5)

$$\nabla^2 \phi^{n+1} = \nabla \cdot (\mathbf{u}^n \times \mathbf{B}^n) \tag{1.6}$$

which is solved in the existing solution procedure [9, 10].

We are easily aware that the relation between the scalar potential and the electric current density in Eq. (1.4) is analogous to that between the pressure and the fluid velocity in Eq. (1.1). In addition, Eqs. (1.2) and (1.5) have the same form, and both Eqs. (1.3) and (1.6) are Poisson

0021-9991/94 $6.00

equations. Therefore the self-correcting procedure would be available also for Eqs. (1.4) to (1.6). But we cannot find a term in Eq. (1.6) that should correspond to the final term in the right-hand side of Eq. (1.3). Eventually the electric current density calculated from Eq. (1.4) could not always satisfy Eq. (1.5) as long as the scalar potential is obtained from Eq. (1.6). This motivated us to apply the self-correcting procedure to magnetohydrodynamic flow.

In the following sections, a new application of the self-correcting procedure to magnetohydrodynamic flow will be described, and then some numerical results obtained by solving an example problem will be shown.

2. DESCRIPTION OF THE PROCEDURE

As already mentioned, there exists an analogy between Eqs. (1.1) and (1.4). However, there also exists a conspicous difference: Eq. (1.1) contains a time derivative, while Eq. (1.4) does not. Therefore a certain substitute for a time derivative should be introduced in Eq. (1.4) so that the self-correcting procedure becomes applicable. In the present application, an underrelaxation is introduced in Ohm's law as

$$\mathbf{J}_t^{k+1} = \sigma(-\nabla\phi^{k+1} + \mathbf{u}^n \times \mathbf{B}^n) \tag{2.1}$$

$$\mathbf{J}^{k+1} = \mathbf{J}^k + \omega_J(\mathbf{J}_t^{k+1} - \mathbf{J}^k) \tag{2.2}$$

where ω_J is the underrelaxation factor $(0 < \omega_J < 1)$, the superscript k's denote the iteration steps, and the subscript t means "tentative." Eliminating $\mathbf{J}_t^{k+1}$ from Eqs. (2.1) and (2.2), we obtain

$$\frac{\mathbf{J}^{k+1} - \mathbf{J}^k}{\omega_J} = -\mathbf{J}^k + \sigma(-\nabla\phi^{k+1} + \mathbf{u}^n \times \mathbf{B}^n). \tag{2.3}$$

It is assumed here that the conservation law of the electric current density is satisfied at the next iteration step $k+1$:

$$\nabla \cdot \mathbf{J}^{k+1} = 0. \tag{2.4}$$

Taking the divergence on both sides of Eq. (2.3), we obtain a Poisson equation for the scalar potential,

$$\nabla^2\phi^{k+1} = \nabla \cdot (\mathbf{u}^n \times \mathbf{B}^n) - \frac{1}{\sigma}\left(1 - \frac{1}{\omega_J}\right)\nabla \cdot \mathbf{J}^k, \tag{2.5}$$

where the final term in the right-hand side is "the self-correcting term." If it is not zero, the scalar potential is corrected so that the electric current density at the next iteration step, $\mathbf{J}^{k+1}$, should satisfy its conservation law, Eq. (2.4). An iterative process of solving Eq. (2.5) for ϕ^{k+1} and calculating $\mathbf{J}^{k+1}$ from Eqs. (2.1) and (2.2) is continued until $|\mathbf{J}^{k+1} - \mathbf{J}^k|$ becomes sufficiently small.

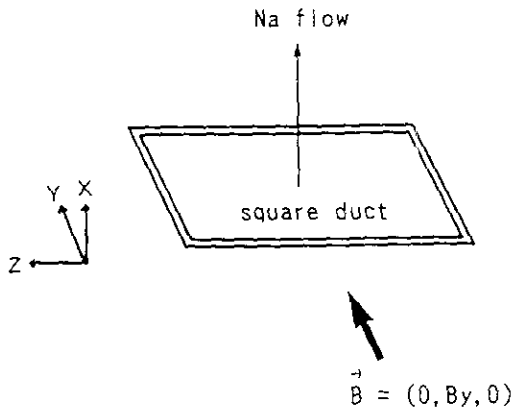

FIG. 1. Schematic drawing of example problem.

The key point in the above procedure lies in applying an iterative computation to Ohm's law and a Poisson equation of the scalar potential. This corresponds to the pressure correction process with the time step advance in the original self-correcting procedure.

3. EXAMPLE PROBLEM

The proposed self-correcting procedure is applied to an example problem. Figure 1 shows a schematic drawing of this problem. In this problem, a fluid velocity distribution in a square duct is solved under a transverse magnetic field, $\mathbf{B} = (0, B_y, 0)$, with the following conditions and assumptions: the working fluid is sodium; the flow is laminar, one-dimensional, and fully developed; the applied magnetic field is uniform and the induced magnetic field is neglected.

Under these conditions, the equation of motion is described as

$$u^{n+1} = u^n + \frac{\Delta t}{\rho}\left(-\frac{dp}{dx} + f_x - J_z^{n+1}B_y\right), \tag{3.1}$$

where u is the x-component of the fluid velocity $\mathbf{u}$.

TABLE I

Analysis Conditions

Reynolds number	$\sim 10^2$ ($\Delta p/\Delta x = -0.18$ kg/m^{2}s^2)
Hartmann number	10^2
Size of the duct	0.03 m × 0.03 m (inner side)
Computational grid	72 × 72 cells (refined in near-wall region)
Wall thickness	0.1 × (half width of the duct)
Time step width	0.01 s
Convergence criteria	0.1 A/m^2 for current density 1.0×10^{-7} m/s for fluid velocity
Initial conditions	1.0×10^{-3} m/s for fluid velocity

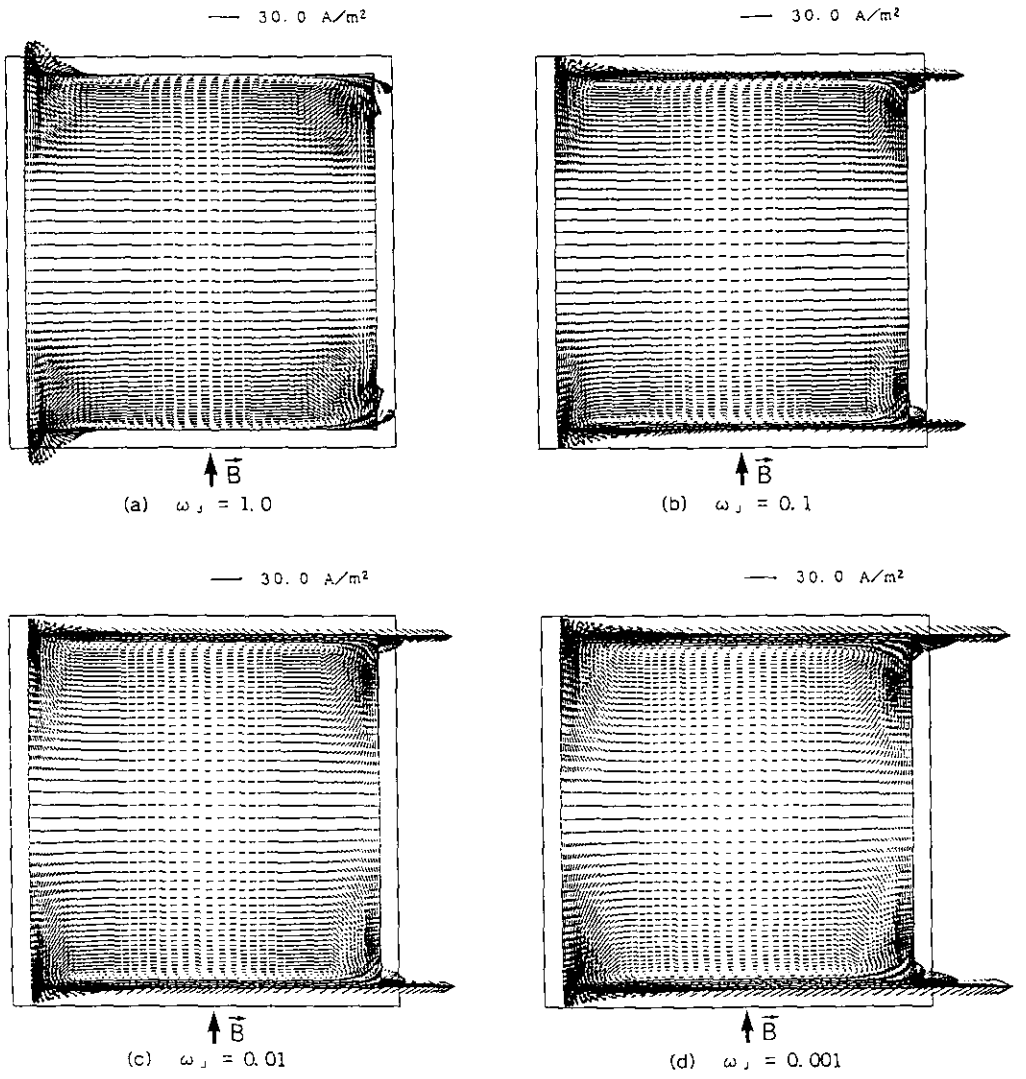

FIG. 2. Electric current density distributions (insulated wall).

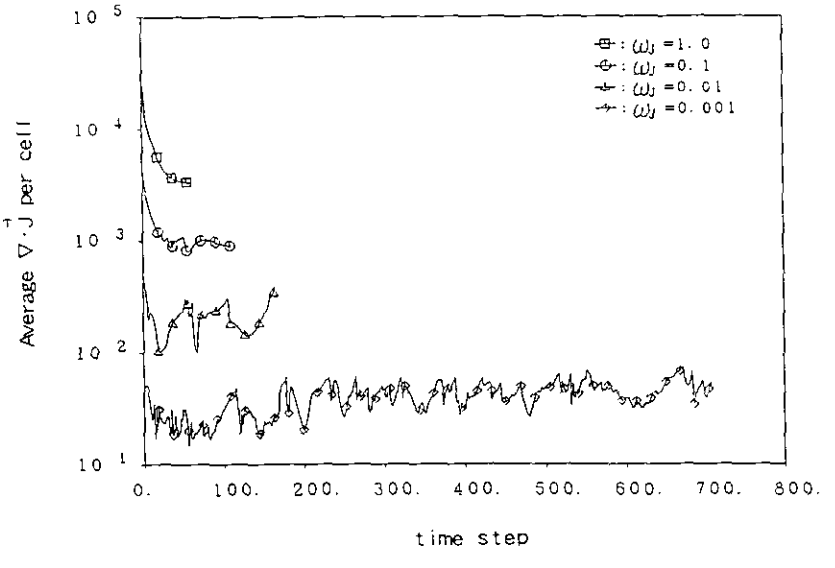

FIG. 3. Trend of average $\nabla \cdot \mathbf{J}$ (insulated wall).

The finite difference method is used to solve this example problem, and the computational grid is staggered one, where the vector quantities are located on cell sides and the scalar quantities are located in cell centers.

The outline of the solution procedure is as follows:

(1) Solve Eq. (2.5) for ϕ^{k+1}.

(2) Calculate $\mathbf{J}^{k+1}$ from Eqs. (2.1) and (2.2).

(3) Repeat the above steps until $|\mathbf{J}^{k+1} - \mathbf{J}^k|$ becomes sufficiently small.

(4) Calculate u^{n+1} explicitly from Eq. (3.1).

(5) Repeat all the above steps until a steady-state velocity field is obtained.

Two cases are treated here for electric property of the duct wall, one is an insulated wall, the other is a conducting wall. The detailed conditions are listed in Table I.

4. NUMERICAL RESULTS

First, some numerical results for the insulated wall are shown. Figures 2a to d show the converged solutions of electric current density distributions obtained for several values of ω_J. When $\omega_J = 1.0$, the self-correcting term is not included in Eq. (2.5). This reflects the numerical result shown in Fig. 2a, where the conservation law of the electric current density is not satisfied well. In fact, the electric currents are turning at the corners of the duct, but we cannot find a return current in the vicinity of the upper and bottom walls in the figure. On the contrary, in Figs. 2b to d, the situations for $\nabla \cdot \mathbf{J}$ seem to be made better by the effect of the self-correcting term.

Figure 3 shows the trend of the average value of $\nabla \cdot \mathbf{J}$ per computational cell. This figure indicates an important fact that the smaller ω_J becomes, the better the conservation law of the electric current density is satisfied.

Figure 4 shows the profiles of the scalar potential along the horizontal center line of the duct. The results in this figure support the results in Figs. 2 and 3: in the case of $\omega_J = 1.0$, the profile of the scalar potential almost flattens, while the gradient becomes so large as to lead the return current as ω_J decreases.

In Figs. 5a to d, the bird's-eye views of the fluid velocity profiles for each ω_J are shown. These figures exhibit how the underrelaxation factor influences the velocity profile. As this factor becomes smaller, the return current and the width of the current path are increased as shown in Figs. 2a to d. Thus the acceleration force in the Hartmann layer increases, whereas Fig. 2 suggests that the stopping force in the core region slightly becomes less as ω_J decreases. This is the reason why so much difference is observed in Figs. 5a to d.

Next, let us move to the case of the conducting wall. This case is taken up in order to demonstrate that the self-correcting procedure is effective also for a solid body. A relevant discussion will be given later. Here the electric conductivity of the wall is the same as that of fluid. Figures 6a to d show the distributions of the electric current density. In Fig. 6a, it is observed that the conservation law of the electric current density is not satisfied in the upper and the bottom walls. On the contrary, this conservation law seems to be satisfied well in Figs. 6b to d. Figure 7 shows the trend of the average value of the $\nabla \cdot \mathbf{J}$ per computational cell. All of these results are similar to those in Figs. 2a to d and Fig. 3.

Figure 8 shows the profiles of the scalar potential along the horizontal center line. The results are similar to those in Fig. 4, except that the profiles in the case of $\omega_J = 0.1$ and $\omega_J = 0.01$ are almost overlapped. This overlapping, however, is not so serious and just corresponds to the nearly equal distributions of the electric current density shown in Figs. 6b and c.

Figure 9 shows the bird's-eye views of the fluid velocity profiles for each ω_J. Similar to Figs. 5a to d, it is confirmed that the velocity profiles are much influenced by the underrelaxation factor also in case of conducting wall.

5. DISCUSSION

The above numerical results demonstrate the effect of the self-correcting procedure in computational magnetohydrodynamics. It is crucial to discuss the relation between the self-correcting procedure and the source term in the Poisson equation of the scalar potential, i.e., $\nabla \cdot (\mathbf{u} \times \mathbf{B})$. In general, both the fluid velocity and the magnetic field are time-dependent variables. This fact leads to a possibility that the source term converges with significant error when the conservation law of the electric current density is not satisfied and the resultant electromagnetic force is not accurate. Then a solution of the scalar potential obtained with such a source term also contains significant error. In this sense, it can be said that the variability of the source term needs some measure to correct the scalar potential, i.e., the self-correcting procedure.

In a computation of the electric current density in a solid body, a Laplace equation of the scalar potential is solved,

$$\nabla^2 \phi = 0. \tag{5.1}$$

We deduce from the above discussion that the self-correcting procedure would not be necessary in this case. And we know that such a procedure is not necessary to solve this type of equation, i.e., a heat conduction equation without a source term. But we should recognize from Figs. 6a to d that when the generation term in the fluid region governs the scalar potential field and the electric current goes into a solid wall, the self-correcting procedure is quite necessary so that the electric current density should satisfy its conservation law.

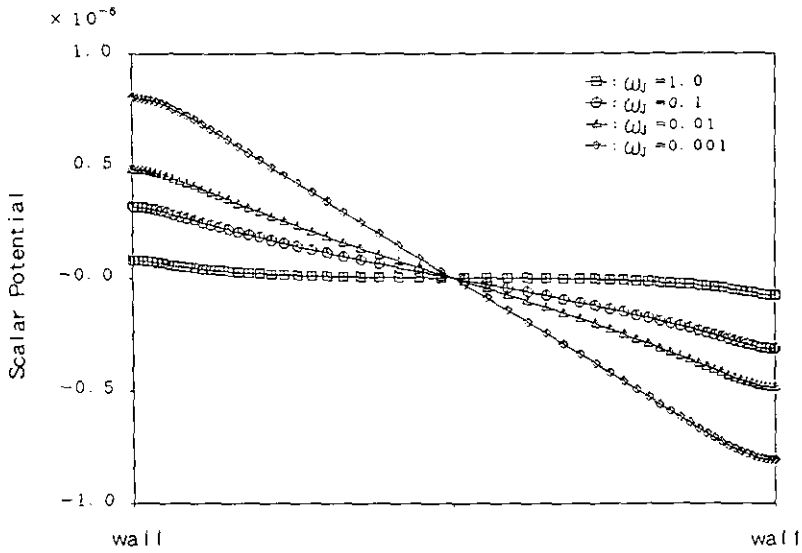

FIG. 4. Scalar potential profiles along the horizontal center line of the duct (insulated wall).

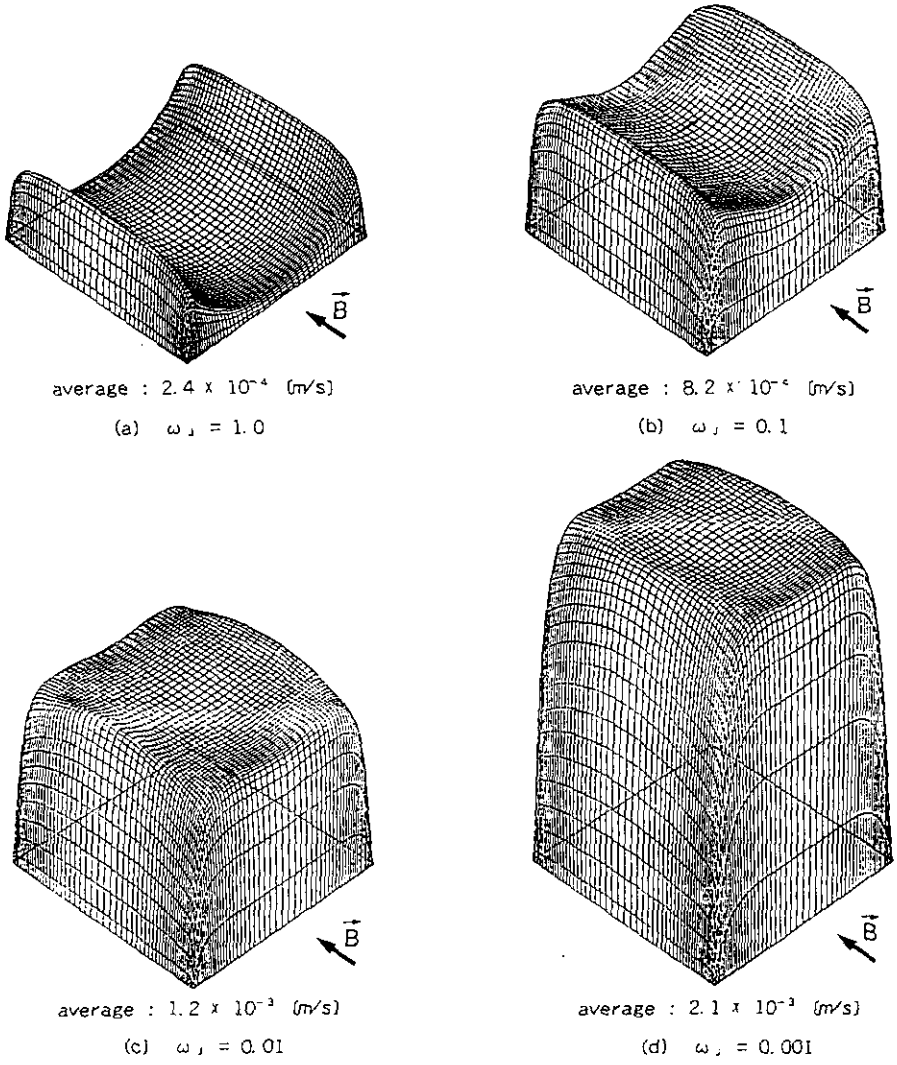

FIG. 5. Bird's-eye views of fluid velocity profiles (insulated wall).

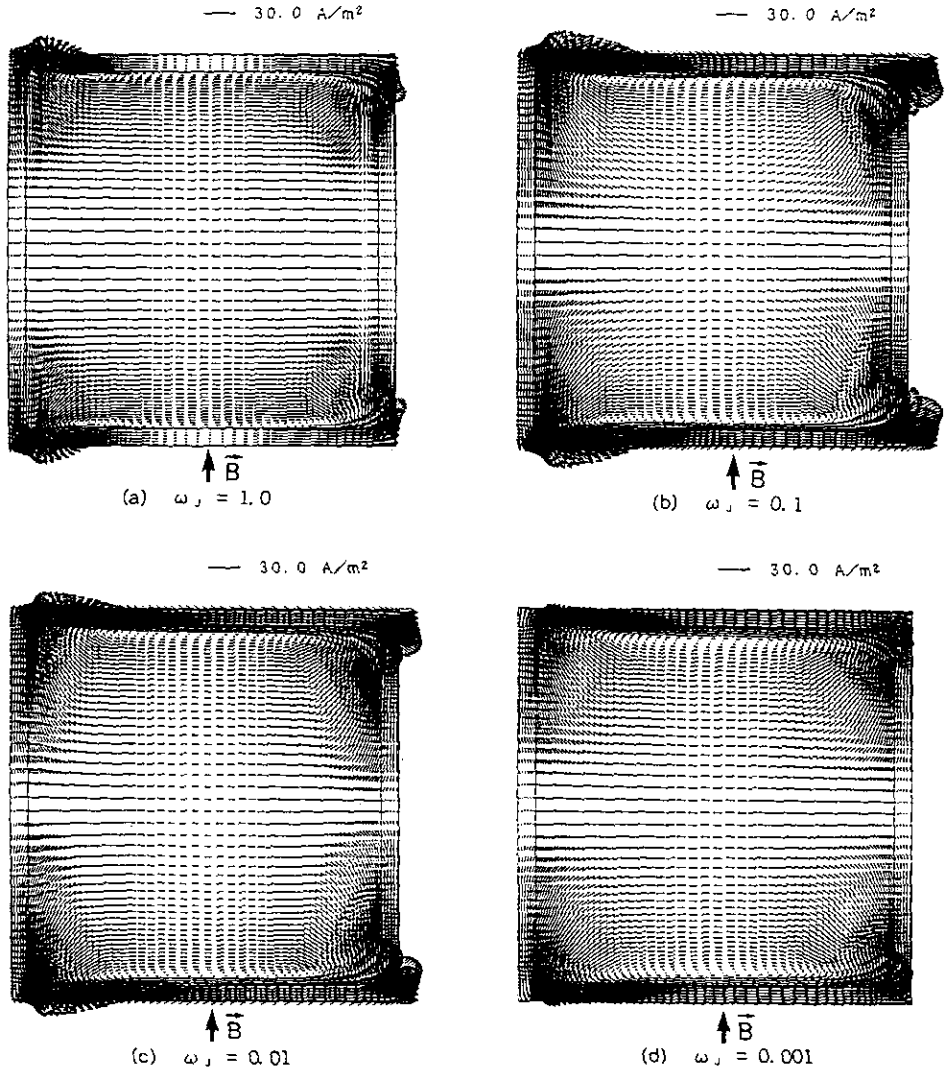

FIG. 6. Electric current density distributions (conducting wall).

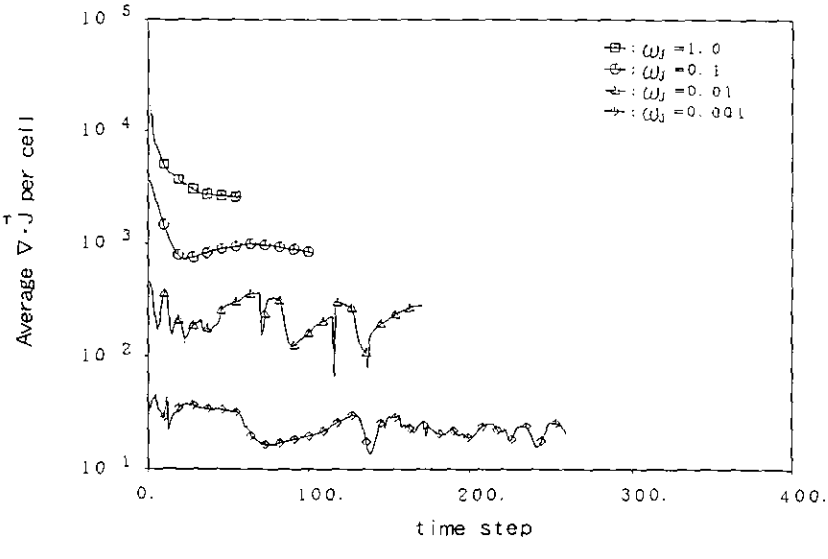

FIG. 7. Trend of average $\nabla \cdot \mathbf{J}$ (conducting wall).

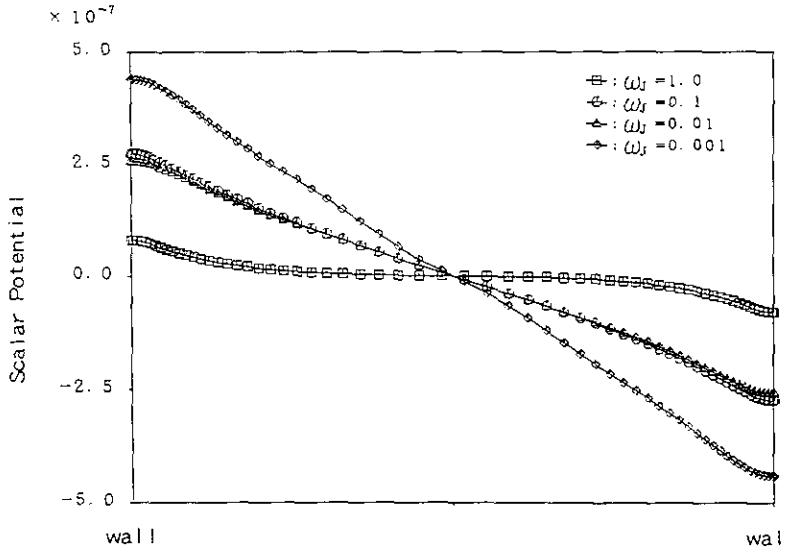

FIG. 8. Scalar potential profiles along the horizontal center line of the duct (conducting wall).

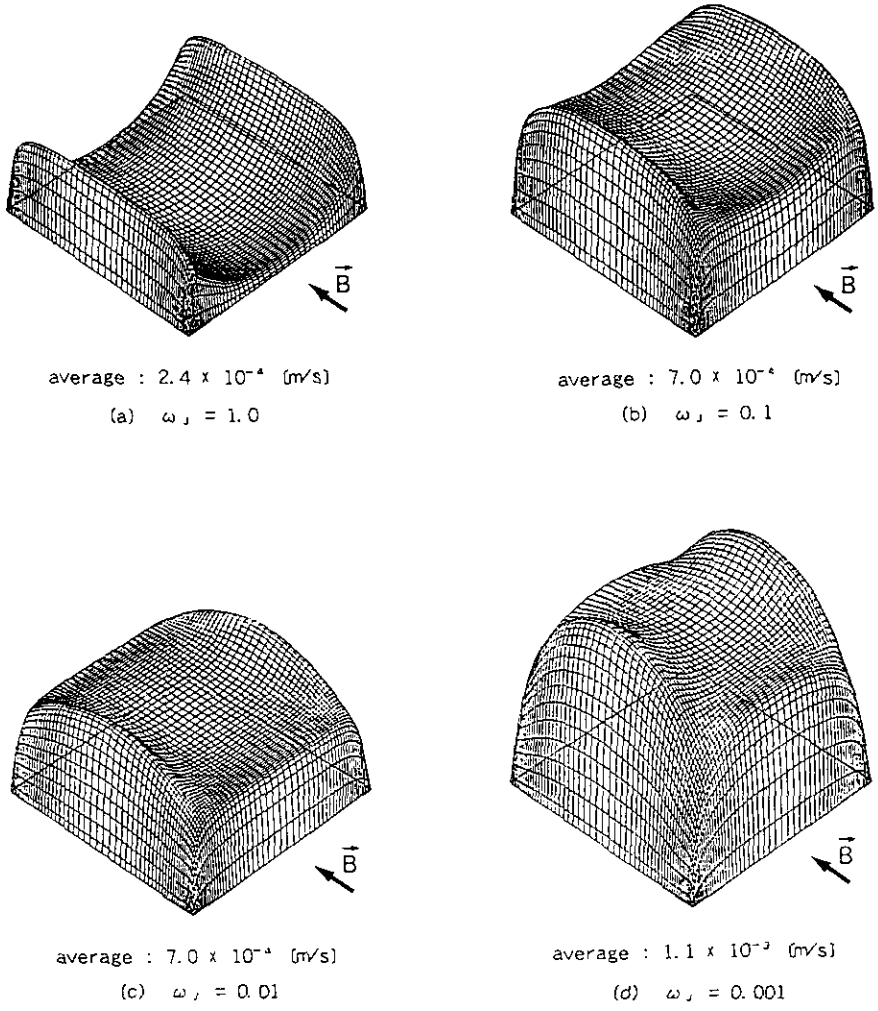

FIG. 9. Bird's-eye views of fluid velocity profiles (conducting wall).

As already mentioned, the remarkable feature of the proposed procedure lies in applying an iterative computation to Ohm's law and a Poisson equation of the scalar potential. One may suppose, however, that the following equation should be solved, instead of Eq. (2.5),

$$\nabla^2\phi^{n+1} = \nabla\cdot(\mathbf{u}^n\times\mathbf{B}^n) + \frac{1}{\sigma}\nabla\cdot\mathbf{J}^n \tag{5.2}$$

which is derived intuitively from Ohm's law and the electric current density should be calculated from Eq. (1.4). In this idea, an iterative computation is not included. In addition, it would be expected that the scalar potential is corrected by the final term in the right-hand side of Eq. (5.2). So this idea seems better than the proposed one. But unfortunately this idea often leads to a numerical solution without convergence. This situation is illustrated in Fig. 10, where the maximum change of the electric current density non-dimensionalized by the average current is plotted along time steps. The result obtained by the above idea shows that the maximum change decreases at early time steps, but begins to increase after that. On the other hand, the result obtained by the proposed procedure decreases gradually with small oscillation. The failure of the above idea is attributed to the following fact: Eq. (5.2) is equivalent to Eq. (2.5) with $\omega_J = 0.5$, while the value of ω_J implicitly included in Eq. (1.4) is unity. Therefore this idea contains an inconsistent relaxation of the electric current density.

It would be important to discuss here about a value of the underrelaxation factor and its influence on a numerical solution. The results shown in Figs. 3 and 7 indicate that the conservation law of the electric current density is satisfied better as ω_J becomes smaller. It should be noted, however, that this tendency does not always mean that an overall accuracy of the numerical solution is improved as ω_J becomes smaller. In other words, when ω_J is too small, there exists a possibility that some trifling value (in the lower places) of $\nabla\cdot\mathbf{J}$, which should be regarded as a numerical error, is amplified by the reciprocal of ω_J. (See Eq. (2.5).) Then the self-correcting term behaves, beyond its original role, as a source term of the scalar potential. In this situation, a numerical solution of the electric current density may satisfy its conservation law well, but it has no basis in physical reality.

Therefore, in order to obtain a numerical solution with physical reality, we have to seek a suitable value of ω_J. Here it must be remembered that an electric conductivity and a computational mesh size are included in the self-correcting term. So, strictly speaking, a suitable couple of ω_J, σ, and a mesh size should be sought for. Thus a further study, which probably accompanies a great deal of work, will be needed in near future.

6. CONCLUDING REMARKS

In this paper, a new application of the self-correcting procedure to liquid metal magnetohydrodynamics was proposed. And it was demonstrated that this procedure is valid to satisfy the conservation law of the electric current density.

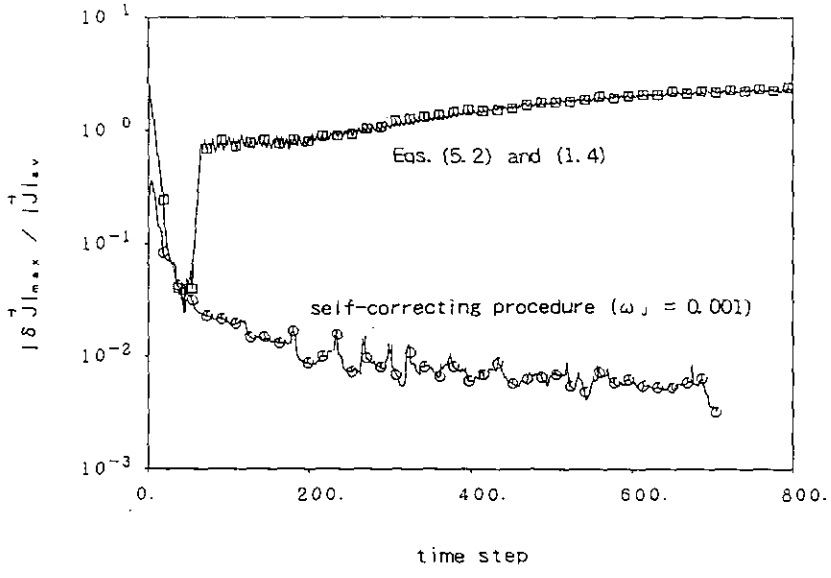

FIG. 10. Maximum change of electric current density non-dimensionalized by average current (insulated wall).

A remarkable feature of the present self-correcting procedure is to apply an iterative computation to Ohm's law and a Poisson equation of the scalar potential with an underrelaxation factor. Some numerical results obtained here show that as the underrelaxation factor becomes small, the conservation law of the electric current density is satisfied better. We have to note, however, that a suitable couple of the underrelaxation factor, an electric conductivity, and a computational mesh size is necessary to obtain a numerical solution with physical reality.

Needless to say, to maintain a physical reality of the numerical solution is an essential requirement in computational magnetohydrodynamics. In this sense, the self-correcting procedure may be no more than a necessary condition, but it is a fundamental numerical technique to satisfy the conservation law of the electric current density.

REFERENCES

1. F. H. Harlow and J. E. Welch, *J. Comput. Phys.* **8** (12), 2182 (1965).
2. J. E. Welch *et al.*, *THE MAC METHOD: A Computing Technique for Solving Viscous, Incompressible, Transient Fluid-Flow Problems Involving Free Surfaces*, LA-3425, 1966 (unpublished).
3. S. V. Patanker and D. B. Spalding, *Int. J. Heat Mass Transf.* **15**, 1787 (1972).
4. C. W. Hirt *et al.*, *SOLA-A Numerical Solution Algorithm for Transient Fluid Flows*, LA-5852, 1975 (unpublished).
5. H. M. Domanus *et al.*, NUREG/CR-3435, ANL-83-64, 1983 (unpublished).
6. G. E. Schneider *et al.*, *Numer. Heat Transf.* **1**, 433 (1978).
7. S. Tuann and M. D. Olson, *Comput. Fluids* **6**, 141 (1978).
8. C. W. Hirt and F. H. Harlow, *J. Comput. Phys.* **1** (2), 114 (1967).
9. C. N. Kim and M. A. Abdou, *Fusion Technol.* **15**, 1163 (1989).
10. A. Sterl, *J. Fluid Mech.* **216**, 161 (1990).